Food Hydrocolloids 114 (2021) 106542

Contents lists available at ScienceDirect

Food Hydrocolloids

journal homepage: http://www.elsevier.com/locate/foodhyd

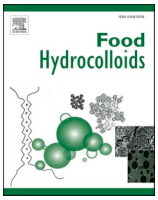

# Evaluation of rennet-induced gelation under different conditions as a potential method for 3D food printing of dairy-based high-protein formulations

Ricardo Uribe-Alvarez [a,b], Norah O'Shea [a,*], Craig P. Murphy [b], Caroline Coleman-Vaughan [b], Timothy P. Guinee [a]

[a] Food Chemistry and Technology Department, Teagasc Food Research Centre, Moorepark, Fermoy, Co. Cork, Ireland
[b] Department of Biological Sciences, Cork Institute of Technology, Bishopstown, Ireland

ARTICLE INFO

*Keywords:*
pH
Temperature.
Rennet gelation
Rheology
3D printing
Milk protein

ABSTRACT

The rennet-induced gelation of milk proteins was evaluated as a potential method for the formation of 3D printed food structures. The effects of pH, [$Ca^{2+}$], and temperature on the rennet gelation properties of milk protein dispersion with 15% (w/w) protein content were assessed using low amplitude strain oscillation rheometry. A cycled-temperature ramp (heating-holding-cooling) during rheological measurements was suitable to evaluate gel firmness development, as an imitation of the temperature profile in the 3D printing process. A factorial design considering two levels of pH (6.0 and 6.4), [$Ca^{2+}$] (1.5 and 5.7 mM), and temperature (31 and 40 °C), showed that the pH, temperature, and its interaction were the main factors enhancing gel formation and the strength of the resultant gel. At pH 6.0 and temperature ramped to 40 °C followed by cooling to 15 °C, a very high gel strength (~8–9 kPa) was obtained. These results showed that rennet-induced gelation could be manipulated for developing printable dairy formulations.

## 1. Introduction

Additive manufacturing (AM), or commonly known as three-dimensional (3D) printing, is a technology where computer designed 3D objects are built by deposition of material(s) in consecutive layers in a single process. The utilisation of food as the printing material is referred to as food layered manufacture or 3D food printing (3DFP) (Godoi, Prakash, & Bhandari, 2016; Liu, Zhang, Bhandari, & Wang, 2017; Wegrzyn, Golding, & Archer, 2012). This technology enables the design of food products with customised nutritional profiles and textures (Godoi et al., 2016; Lipton, Cutler, Nigl, Cohen, & Lipson, 2015; Liu et al., 2017; Wegrzyn et al., 2012). Different 3D printing methods have been tested using food materials. These can be classified into three main groups: (1) extrusion, (2) powder liquid/hot air/laser binding, and (3) inkjet printing (Godoi et al., 2016; Liu et al., 2017). The extrusion method is the most common used for 3DFP. This technique extrudes a viscoelastic food formulation from the printer nozzle, which solidifies immediately on deposition and fuses to the previous layer (Sun, Zhou, Yan, Huang, & Lin, 2018). Food materials that have been successfully printed using this technique include dough, mashed potatoes, cheese, and meat paste (Godoi et al., 2016; Le Tohic et al., 2018; Lipton et al., 2010).

Milk proteins are potentially viable ingredients for 3DFP using the extrusion method, due to the structure-forming capabilities of the proteins upon gelation, which is then appropriate for building 3D objects (Liu et al., 2018; Ross, Kelly, & Crowley, 2019; Schutyser, Houlder, de Wit, Buijsse, & Alting, 2018). Recent studies have reported on 3DFP using skimmed milk powder (Derossi, Caporizzi, Azzollini, & Severini, 2018), semi-skimmed milk powder (Lille, Nurmela, Nordlund, Metsä-Kortelainen, & Sozer, 2018), sodium caseinate (Schutyser et al., 2018), processed cheese (Le Tohic et al., 2018), blends of milk protein concentrate (MPC) and whey protein isolate (WPI) (Liu et al., 2018), and sodium caseinate and MPC (Liu et al., 2019). The gelation of the milk proteins produced the 3D structure formation in these studies, triggered by heating, increasing protein concentration, synergy with hydrocolloids, or combinations of these. Interestingly, none of these studies used rennet-induced gelation.

Both types of milk proteins, casein and whey, can form a gel but

* Corresponding author.
*E-mail address:* norah.oshea@teagasc.ie (N. O'Shea).

https://doi.org/10.1016/j.foodhyd.2020.106542
Received 28 August 2020; Received in revised form 9 December 2020; Accepted 10 December 2020
Available online 15 December 2020

using different mechanisms. Casein gelation is a very well-studied topic as it is an essential step in the cheese-making process. Casein gels can be formed by selective hydrolysis of the micelle-stabilising protein, κ-casein, from the surface of the casein micelles by aspartyl proteinases (rennets), acidification to the isoelectric pH (~4.6) of casein, or a combination of both (Lucey, 2002; Van Vliet, Lakemond, & Visschers, 2004). Rennet-induced gelation can be divided into two phases, a primary stage involving the hydrolysis of κ-casein, and a secondary stage involving the aggregation and gelation of the rennet-altered micelles (Corredig & Salvatore, 2016; Fox, Guinee, Cogan, & McSweeney, 2017; Lucey, 2002). Several factors (i.e., protein and fat content, heat treatment applied to milk, ionic strength, temperature, pH, and rennet concentration) can affect one or both phases, altering the rennet-induced gelation time and strength of the resulting gel (Fox et al., 2017).

Milk protein concentrates (MPCs) have the same casein-to-whey protein ratio as milk and, therefore, can be used for total or partial milk replacement of milk in dairy-based foods, or as a protein fortification ingredient in food formulation (Agarwal, Beausire, Patel, & Patel, 2015). As an ingredient, MPC is a high-value ingredient due to its nutritional content (high protein and low lactose content) and functional properties (viscosity, gelling, and emulsification) (Agarwal et al., 2015). Increasing the protein content of milk with MPC, while maintaining the rennet-to-total protein ratio constant, reduces the rennet gelation time and increases the gel strength (Guinee, O'Kennedy, & Kelly, 2006).

The rheological properties of milk rennet-induced gels can be determined by dynamic low amplitude oscillation using a controlled strain or stress rheometer (Fox et al., 2017). The main gelation parameters determined in the rennet coagulation are storage modulus (G'), loss modulus (G''), and tan delta, which is the ratio of the G'' to G' (Lucey & Singh, 1997). In cheese making, G' is considered as an index of the gel firmness at a specific time after rennet addition. Rheology is an essential tool for extrusion of 3DFP as it enables the evaluation of parameters (i.e., printability, applicability, and post-processing stability) which are critical to the design of the final 3D food structure formed (Godoi et al., 2016; Zhu, Stieger, van der Goot, & Schutyser, 2019). For example, Kern, Weiss, and Hinrichs (2018) reported 60 °C as the melting temperature of semi-hard model cheese at different pH and calcium/-protein ratios using small amplitude oscillatory temperature sweep measurements, to simulate the holt-melt extrusion 3D printing in a capillary rheometer.

The objective of the current study is to assess a milk protein isolate-fortified-milk dispersion (15%, w/w protein) as a printable formulation by the adoption of the rennet induced gelation process to 3DFP using low amplitude strain oscillation rheometry. The following conditions were varied to alter gelation kinetics and the strength of the resultant rennet-induced gel: calcium ion concentration ($[Ca^{2+}]$), pH, and temperature profile during measurement. A cycled-temperature ramp (involving heating/ramping, holding, and cooling) was used to simulate the typical changes in temperature during 3D printing and the resulting impact on the rheological properties of the gel formed. The identified formulation and conditions will be used as a starting point for developing a 3D food grade printer.

## 2. Materials and methods

### 2.1. Milk powder ingredients

Low heat skim milk powder (LHSMP) and milk protein isolate (MPI) (Ultranor™9075) were obtained from Ornua (Dublin, Ireland) and Kerry Group (Tralee, Co. Kerry, Ireland), respectively.

### 2.2. Compositional analysis of milk powder ingredients

LHSMP and MPI powder were analysed for fat by Rose-Gottlieb (ISO, 2008) in duplicate and total protein by Kjeldahl (ISO, 2014) in triplicate. For lactose, individual casein and whey proteins determination, LHSMP and MPI were reconstituted by dispersing to 10% (w/w) and 4% (w/w) respectively, in distilled water at 50 °C while stirring at 800 rpm for 1 h (IKA RT10 magnetic stirrer, IKA-Werke GmbH & Co. KG, Staufen, Baden-Württemberg, Germany). Post reconstitution, the samples were stored in a refrigerator at 4 °C overnight.

The individual proteins were analysed by reversed-phase high-pressure liquid chromatography (RP-HPLC; Agilent 1200 series, Agilent Technologies, Santa Clara, CA, USA) using a 300 SB-C18 RP Poroshell column (Agilent Technologies), as described by Lin, Kelly, O'Mahony, and Guinee (2016). The protein calibration standards used for RP-HPLC analysis included $\alpha_s$-casein, β-casein, κ-casein, α-La, and β-Lg. Briefly, the samples were diluted in a dissociating buffer containing 7 M urea, 0.02 M Bis-Tris propane, and 0.5% (v/v) 2-mercaptoethanol before injection onto the column. The volume ratio of the reconstituted milk protein ingredient to the dissociating buffer was 1:20, and the sample volume injected onto the column was 10 μL. Samples were analysed in duplicate.

Lactose was separated and quantified using an Aminex HPX 87C Carbohydrate column (300 × 7.8 mm; fixed ion resin column) (Bio-Rad laboratories, Deeside, UK) as described by Morrin et al. (2019). Briefly, the column was set at 60 °C, and the eluent 0.009 N $H_2SO_4$ was run at 0.5 mL/min, and lactose was detected using a refractive index detector (Waters Corporation, Milford, Massachusetts, USA). Calibration curves were prepared using lactose solutions with concentrations of 10, 20, 50, and 100 μg/mL, prepared from a lactose standard (Merck, Darmstadt, Germany). Samples were analysed in duplicate.

### 2.3. Preparation of milk protein dispersions

Firstly, a skim milk (SM) base was prepared by dispersing LHSMP (10% w/w) in distilled water at 50 °C while stirring at 6000 rpm for 5 min using a high shear mixer (Silverson model L4RT, Silverson, Chesham, UK). The appropriate quantity of MPI was added to the SM base, to give the desired final protein content of 15% (w/w). The blend of MPI and SM base was manually mixed for at least 15 min until all powder was wetted. Then the mixture was placed in a water bath set to 50 °C and stirred for 20 min at 500 rpm using an overhead stirrer (Model RW16; IKA-Werke GmbH, Staufen im Breisgau, Germany). Next, the suspension was high shear mixed at 7000 rpm for 6 min until a uniform dispersion free of visual powder agglomerates was formed. After high shear mixing, the milk protein dispersion was stirred for a further 2 h at 500 rpm using an overhead stirrer at room temperature. After stirring, a foam layer that had formed was discarded by decantation. A milk preservative (Broad Spectrum Micro Tabs, D & F Control Systems Inc., California, U.S.A.) was added at a level of one tablet per 40 ml of the sample before storing overnight at 4 °C. For all assays, samples of milk protein dispersions were warmed at 40 °C for 30 min before assaying, to reverse cold-ageing effects (Dalgleish & Law, 1988).

### 2.4. Compositional analysis of milk protein dispersions

Milk protein dispersions were diluted 4-fold in distilled water for protein determination using the Fourier transform infrared Bentley FTS (Bentley Instruments Inc., Chaska, USA). The concentration of ionic calcium, $[Ca^{2+}]$, was measured after equilibrating the samples at 25 °C, using the sensION+ 9660C calcium combination ion-selective electrode (Hach Lange, Barcelona, Spain). Potassium chloride (3 M) was added to the samples at a level of 1% (v/v) and the $[Ca^{2+}]$ was measured while stirring. The electrode calibration was performed using $CaCl_2$ solutions (0.0, 0.5, 2.5, 5.0, and 10.0 mM) as described by Lin et al. (2016).

### 2.5. Solubility of milk protein dispersions

The solubility of the milk protein dispersions after storage at 4 °C, was determined as the percentage solubility using a modification of the

method described by Gazi and Huppertz (2015). Briefly, the milk protein dispersions were diluted in distilled water to a protein concentration of ~3.5% (w/w), centrifuged at 700×*g* for 10 min at 25 °C. The percentage of solubility was calculated as the percentage of total solids (TS) in the supernatant divided by the percentage of TS in the original dispersion. The TS were measured using the CEM SMART Trac II (CEM Corp., Charlotte, NC).

### 2.6. Rennet gelation

A two-level full factorial design with three factors ($2^3$) was used to evaluate the effect of pH (6.0 and 6.4), [$Ca^{2+}$] (1.5 and 5.7 mM), and temperature (31 and 40 °C) on the rennet gelation properties. Three replicates were carried out at each setting, and a letter was assigned per treatment, as shown in Table 1. The high pH value (6.4) corresponded to the milk protein dispersion (with no pH adjustment), and the low value (6.0) was obtained on adjusting the dispersion with 1 N HCl at 25 °C. The pH value of 6.0 was chosen as it is known to enhance both the enzymic and coagulation phases of rennet gelation (Fox et al., 2017). The lowest level of [$Ca^{2+}$] corresponds to the initial concentration of the milk protein dispersion and the higher level was obtained after the addition of $CaCl_2$ (Sigma-Aldrich, Saint Louis, US) to adjust the [$Ca^{2+}$]: casein ratio to that of the reconstituted LHSMP. $CaCl_2$ was added directly to the samples before rheological measurement, and any drop in the pH was reversed by the addition of 0.1 N NaOH.

The rennet gelation properties of milk protein dispersion samples prepared as per Table 1 (i.e., pH, temperature, and [$Ca^{2+}$]) were measured using a controlled strain rheometer (MCR 302, Anton Paar, Austria), equipped with a cup and bob geometry (CC27) with radius 28.92 and 26.66 mm, respectively, as described by Guinee et al. (2006). Chymosin (Chy-Max® Extra, 600 IMCU $mL^{-1}$; Chr. Hansen, Hørsholm, Denmark), diluted 20-fold with distilled water, was added at a level of 500 μL per 100 g of milk protein dispersion. The storage modulus (G') and loss modulus (G'') were measured dynamically as a function of time over 1 h at a strain of 0.025 and a frequency of 1 Hz (Lin et al., 2016). The strain applied is within the linear viscoelastic region for measuring rennet gelation properties (Fox et al., 2017; Zoon, Van Vliet, & Walstra, 1988a). To prevent evaporation from the samples, the surface was covered with vegetable oil.

The following rennet gelation properties were obtained from the resultant G'/time curves: gelation onset time (GOT), gel point (GP), maximum gelation rate (MGR), time to MGR ($t_{MGR}$), and the final G' value of the gel formed ($G'_F$). GOT was calculated as the time when G' = 1 Pa, GP as the time when G' = G'', MGR as the maximum slope of the G'/time in kPa $min^{-1}$, and $t_{MGR}$ as the time to reach the MGR.

Two different temperature control methodologies were used in this study. The first method is referred to as constant-temperature mode; in this approach, all samples were equilibrated to the test temperature prior to rennet addition and maintained during the rheological measurement. With this method, the GOT and GP parameters at 40 °C and pH = 6.0 (treatments E and F) occurred before the first reading on the rheometer. The second method, referred to as cycled-temperature ramp, involves the application of a temperature cycle, whereby rennet was mixed with the milk protein dispersion at 25 °C for 30 s before loading onto the rheometer. Once loaded, the temperature was held at 25 °C for 2 min, it was then increased to the gelation temperature (31 or 40 °C) at a rate of 5 °C $min^{-1}$, held at 31 or 40 °C for 30 min, and reduced at a rate of 1.8 °C $min^{-1}$ to 15 °C (Figure S1). This method enabled the detection of gelation transition under all the experimental conditions (Table 1). It is envisaged that the cycled-temperature ramp approach will also simulate the temperature cycle likely to be used during 3D printing. For measurements performed using the cycled-temperature ramp, the MGR was determined during the holding stage of the cycle.

**Table 1**
Values of factor variables of each coded treatment of the experimental design.

| Treatment | Temperature (°C) | pH | [$Ca^{2+}$] (mM) |
|---|---|---|---|
| A | 31 | 6.0 | 1.5 |
| B | 31 | 6.0 | 5.7 |
| C | 31 | 6.4 | 1.5 |
| D | 31 | 6.4 | 5.7 |
| E | 40 | 6.0 | 1.5 |
| F | 40 | 6.0 | 5.7 |
| G | 40 | 6.4 | 1.5 |
| H | 40 | 6.4 | 5.7 |

### 2.7. Statistical analysis

Shapiro–Wilk and Levene tests were used to check the normality and homoscedasticity assumptions, respectively. The data were analysed using a one-way analysis of variance (ANOVA) with a pairwise multiple comparison procedure (Tukey-Test) for testing differences of the gelation properties between all treatment means. The effect of the factors on each response variable for the measurements made using the cycled-temperature ramp was determined using a three-way ANOVA. Statistical analysis was performed using the software RStudio Version 1.1.463 (RStudio, Inc). Differences were identified as significant at $p < 0.05$.

## 3. Results and discussion

### 3.1. Composition of dairy ingredients and milk protein dispersion

The protein content for the LHSM and MPI was 32.8 ± 0.3 and 85.0 ± 0.1% (w/w), respectively. The proportions of individual caseins and whey proteins were typical of those previously reported for bovine milk (Gulati et al., 2019; Lin et al., 2016). Similarly, the fat and lactose content (Table S1) were also typical of that found in literature (Augustin & Clarke, 2011; Singh, 2009). The mean protein content of the control milk protein dispersion was 15.70 ± 0.39% (w/w), slightly higher than the target value (15%). This higher protein content could be related to partial evaporation of the dispersion during mixing at 50 °C.

It is well known that dairy powders with high casein content are difficult to hydrate. However, skim milk has been reported to improve MPC solubility compared to water (Udabage, Puvanenthiran, Yoo, Versteeg, & Augustin, 2012). Therefore, reconstituted LHSM was used as the solvent to hydrate MPI. The solubility of the control dispersion was 94.7 ± 1.1%. To the best of the authors' knowledge, no studies have reported on the solubility of milk dispersions with protein content >10% (w/w). Using a similar method of preparation and solubility measurement as that in the current study, Bot, Crowley, O'Mahony (2020), reported solubility of 90.1–92.3% of milk protein dispersions with 8.5% protein content prepared by mixing dispersions of reconstituted MPI and sodium caseinate (NaCas). An examination of the literature indicates a slight variation in protein solubility in milk protein dispersions prepared from MPI, probably due to differences in the method of MPI manufacture (e.g., milk heat treatment, the extent of diafiltration, lactose content, ionic strength), the solvent used for reconstitution (e.g., LSHM, NaCas) and the conditions used to reconstitute MPI, i.e., temperature, shear and time. The solubility data from the current study indicate that the use of skim milk as a solvent and the method of reconstitution, i.e., high and low-shear mixing combination followed by 4 °C overnight storage, was an appropriate method to achieve a high protein (~15%) dispersion with acceptable solubility (~95%).

The control milk protein dispersion had a pH of 6.4 ± 0.1 and [$Ca^{2+}$] of 1.5 ± 0.3 mM. The latter parameter was similar to that of the SM base (1.4 mM). This minimum difference on the [$Ca^{2+}$] can be explained based on the fact that in the MPI process most soluble salts are removed, and a small number of counter-ions are bounded to the negatively-charged proteins (Crowley, Boudin, et al., 2015). Besides, the reconstituted LHSM contains salts (e.g., cit-rate) that can complex ionic calcium ions, which might be contributing to reduce the [$Ca^{2+}$] in the serum phase (Crowley, Desautel, et al., 2015). Furthermore, on lowering

the pH to 6.0, the [$Ca^{2+}$] increase to 2.9 ± 0.2 mM. This increase is consistent with the higher degree of solubilisation of colloidal calcium phosphate (CCP) by the pH drop, consequentially increasing the [$Ca^{2+}$] in the serum phase (Crowley, Boudin, et al., 2015; Dalgleish & Law, 1989).

### 3.2. Rheological properties of rennet-treated milk protein dispersions

Ideally, printable food formulations for extrusion-based 3DFP should have relatively low viscosity to be extrudable through a narrow nozzle, and sufficient mechanical strength to support a load of consecutive deposited layers without buckling/collapsing (Liu, Bhandari, Prakash, Mantihal, & Zhang, 2019). From previous experiments, it was established that a 15% protein (w/w) milk dispersion with a chymosin: protein ratio similar to that used in cheese manufacture (1000 IMCU kg protein$^{-1}$) had suitable viscoelastic properties for potential use as a printable dairy formulation. Therefore, the rennet gelation properties of the milk protein dispersion under different conditions of temperature, pH, and [$Ca^{2+}$] were investigated to determine which combination of factors promote gelation properties for potential use in 3DFP.

On developing printable dairy formulations, rheological measurements collected during a temperature sweep (heating or cooling) are used to characterise the sol-gel transition of the edible material and establish the 3D printing process's temperature parameters (Kern et al., 2018; Le Tohic et al., 2018; Schutyser et al., 2018). Hence, a cycled-temperature ramp, involving heating, holding and cooling, was applied in the current study to compare the effects of varying the temperature during gelation as opposed to holding the temperature constant, as it is typical in most studies, which investigate the rennet gelation characteristics of milk.

The effects of changing the temperature, pH, and [$Ca^{2+}$] of the milk protein dispersions on the development of G' over time performed at constant- and cycled-temperature experiments are shown in Fig. 1. For the constant-temperature measurements, illustrated in Fig. 1a & b, all profiles showed three phases, namely: a lag phase representing the enzymatic hydrolysis of κ-casein from the micelles; an exponential phase in which the micelles have most of their κ-casein removed (i.e.,> 97%), i.e., para-casein micelles, undergo rapid fusion/aggregation, resulting in gel formation; and finally, a stationary (plateau) stage coinciding with the hydrolysis of the remaining κ-casein from the micelle surfaces, and further fusion between the surfaces of aggregated para-casein micelles (Dalgleish, 1983; Walstra & Van Vliet, 1986). A notable difference with

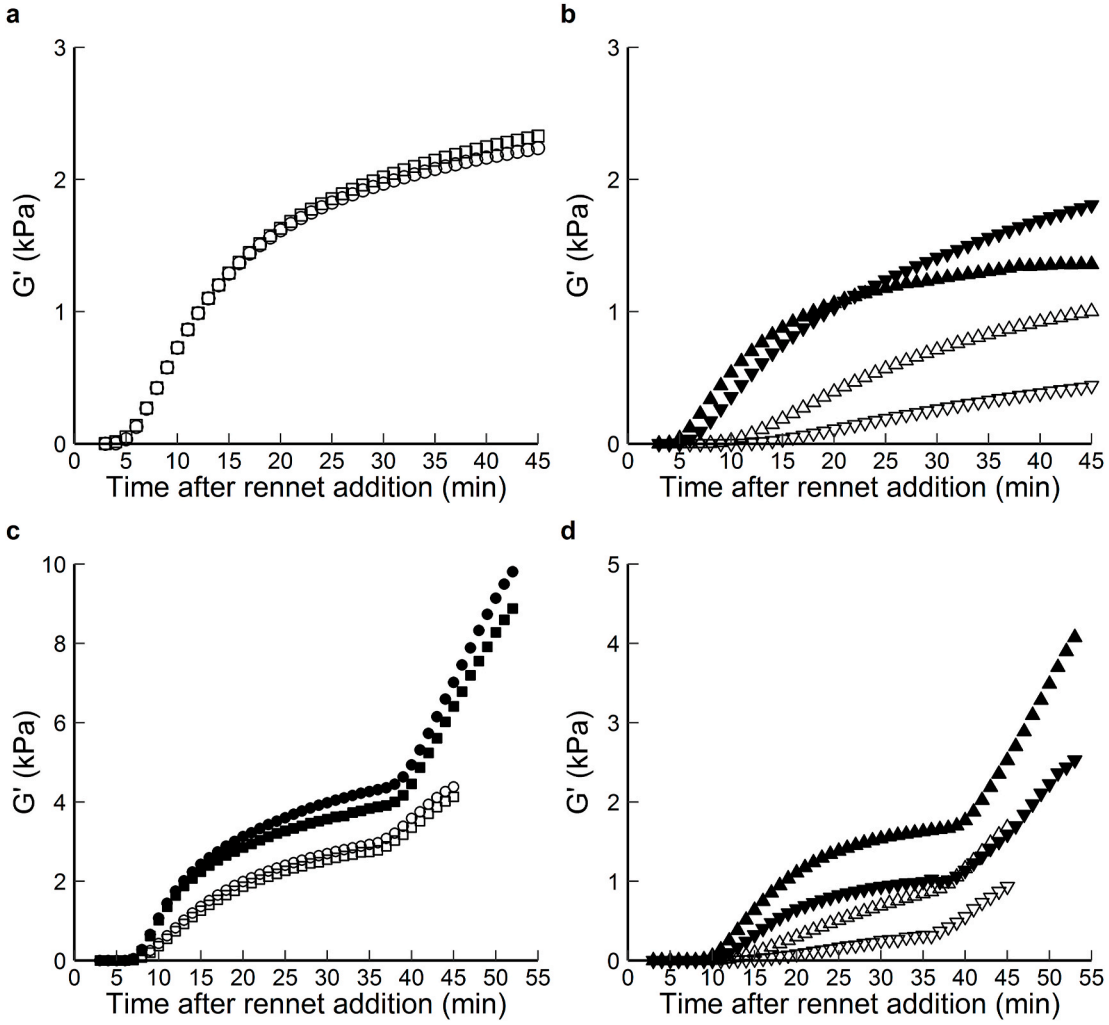


**Fig. 1.** Development of storage modulus (G') of rennet-treated milk protein dispersions as a function of time when using constant-temperature mode (a and b) and cycled-temperature ramp (c and d) measurement. For the cycled-temperature ramp measurements, the temperature was increased from 25 °C to the test temperature (31 or 40 °C) at a rate of 5 °C min$^{-1}$, held at 31 or 40 °C for 30 min, and cooled to 15 °C at a rate of −1.8 °C min$^{-1}$. For both assays, measurements at pH of 6.0 and 6.4 are on the left (a and c) and right (b and d) side, respectively. Temperatures of 31 and 40 °C are denoted by open and closed symbols, respectively. [$Ca^{2+}$] of 1.5 mM is de-noted by squares and down-point-ing tri-an-gles, and 5.7 mM by circles and up-pointing triangles. The treatment dispersions (A–H) are identified as follows: A (□), B (○), C (▽), D (△), E (■), F (●), G (▾), H (▲). Presented data for each treatment are the means of triplicate samples.

the temperature cycling ramp measurements, illustrated in Fig. 1c & d, was the occurrence of a fourth phase, i.e., an increase in G' on cooling from 31 or 40 °C to 15 °C at a rate of −1.8 °C $min^{-1}$, with the effect being more pronounced for 40 °C. Measurements at 31 and 40 °C reach 15 °C at 45 and 53 min after rennet addition, respectively. The increase of the G' during the cooling stage agrees with previous studies on the rheological effect on lowering the temperature of rennet gels (Sinaga, Bansal, & Bhandari, 2017; Zoon, Van Vliet, & Walstra, 1988b). Zoon et al. (1988b) attributed this effect to the swelling of the casein micelles, as a response to the decrease of hydrophobic interaction within the micelles due to a temperature decrease. Moreover, the swelling of micelles increases the contact area between them, increasing the inter-micelles interactions (i.e., hydrogen bonding) that contribute to a higher G' (Lucey, Teo, Munro, & Singh, 1997; Zoon et al., 1988b).

With the constant-temperature mode of measurement, samples at low pH (6.0) and a high temperature (40 °C) (treatments E and F), had already gelled at the beginning of the measurement, as evidenced by the fact that G' exceeded G'' in the first reading (data not shown). This observation is consistent with the strong effect of temperature on the aggregation rate of para-casein micelles (Dalgleish, 1983), well known of the high $Q_{10}$ factor (~16) above 18 °C in rennet coagulation (Fox et al., 2017); therefore the dramatic effect of temperature (40 °C) on the gel properties is not surprising. Hence, the application of the cycled-temperature ramp was used to characterise the sol-gel transition using the previous conditions mentioned.

A notable feature on the development of G' over time for both modes of temperature was the interaction effect of pH, temperature and $[Ca^{2+}]$. It appears that increasing the $[Ca^{2+}]$ from 1.5 mM to 5.7 mM affects the G' profile for treatments with high pH (6.4). However, at the low pH (6.0) the G' development seems not to be influenced by increasing the $[Ca^{2+}]$. Also, the low pH (6.0) and high temperature (40 °C) appear to increase G' values compared to the high pH (6.4) and low temperature (31 °C).

The values of GOT (data not shown) and GP were similar for all treatments within each temperature mode, apart from the values with a high pH (6.4) and a low temperature (31 °C) (treatments C and D), where the difference was greater than 1 min. This similarity may be explained by the high protein content of the dispersions, and hence, the high volume fraction of casein micelles, which led to a large number of binding sites for network formation (Horne & Lucey, 2017). Therefore, once the gel onset started (G' = 1 Pa), the time to reach the stage of gelation where G' = G'' was short, as a network could be created shortly after rennet addition. Samples with a high pH (6.4) and a low temperature (31 °C) (treatments C and D) did not follow this trend as a higher temperature, or a lower pH is needed to enhance the enzymatic hydrolysis and the coagulation rate of κ-casein and para-casein micelles, to induce a rapid gel network. As the starting temperature and heating rate are the same for treatments with the cycled-temperature ramp, the GOT for this method was not significantly affected by temperature, whereas it was significantly reduced by lowering pH from 6.4 to 6.0 and increasing $[Ca^{2+}]$ from 1.5 to 5.7 mM (Table 2).

It is observed in Fig. 2a that all the GP values occurred earlier when operating in constant-temperature compared to the cycled-temperature ramp, this delay is expected as the former mode has a longer lag phase, and it is more visible when transforming G' values to a logarithmic form (Figure S2). This tendency is attributed to the higher starting temperature of the former, i.e., 31 or 40 °C versus 25 °C, as higher temperatures promote more rapid rennet activity and acceleration in the rate of collisions between para-casein micelles reducing the time of gelation significantly (Mishra, Govindasamy-Lucey, & Lucey, 2005). The combination of high pH (6.4), low temperature (31 °C), and low $[Ca^{2+}]$ (1.5 mM) (treatment C) showed to have a significant longer GP in both temperature modes compared to most of the other treatments. This observation is consistent with the literature, showing that a lower pH or higher $[Ca^{2+}]$, enhanced aggregation and gelation of para-casein micelles (Corredig & Salvatore, 2016; Fox et al., 2017).

**Table 2**
Significance levels of the three-way ANOVA for the effects of the pH, $[Ca^{2+}]$ and temperature of the cycled-temperature ramp measurements.[a]

| Factor | Gel onset time | Gelation point | MGR | $t_{MGR}$ | $G'_F$ |
|---|---|---|---|---|---|
| pH | ** | *** | *** | *** | *** |
| $[Ca^{2+}]$ | * | * | *** | NS | *** |
| Temperature | NS | NS | *** | *** | *** |
| pH × $[Ca^{2+}]$ | NS | * | NS | NS | NS |
| pH × Temperature | NS | NS | *** | *** | *** |
| $[Ca^{2+}]$ × Temperature | NS | NS | NS | NS | NS |
| pH × $[Ca^{2+}]$ × Temperature | NS | NS | NS | NS | NS |

[a] Abbreviations are: NS, not significant; MGR, maximum gel rate; $t_{MGR}$, time to maximum gel rate; $G'_F$, final value of storage modulus measured. Each factor was evaluated at two levels of pH (6.0 and 6.4), $[Ca^{2+}]$ (1.5 mM and 5.7 mM), and temperature (31 and 40 °C). Data correspond to 8 treatments, with 3 triplicates per treatment. Significance: *, $p < 0.05$; **, $p < 0.01$; ***, $p < 0.001$.

As mentioned before in this section, gel transition at low pH (6.0) and high temperature (40 °C) (treatment E and F) for constant-temperature mode measurements occurs quite fast, and it was not possible to determine the GP with this combination. It is expected that the GP of these samples occurred within 2 min of rennet addition, as this was the average time required for the sample to be loaded onto the rheometer. These conditions could be suitable for co-extrusion 3D printing, where a concentric nozzle is used to convey and deposit two different materials, for example, the milk protein dispersion and rennet solution, which upon deposition, blend and undergo rapid gelation. Co-extrusion 3D printing has been applied successfully for printing pectin-based food structures by co-extrusion of pectin and $CaCl_2$ solutions (Vancauwenberghe, Verboven, Lammertyn, & Nicolaï, 2018).

For cycled-temperature measurements, a high pH (6.4), low temperature (31 °C) and low $[Ca^{2+}]$ (1.5 mM) (treatment C) delayed the GP in a significant way compared to the other conditions, except at the same pH and $[Ca^{2+}]$ but at 40 °C (treatment G). This trend is associated with the same starting temperature (25 °C) for all treatments when applying the cycled-temperature ramp. Consequently, only pH and $[Ca^{2+}]$, separately or combined, had a significant effect on the GP, as shown by the ANOVA analysis (Table 2).

At low pH, the G'/time profile of treatments at the same temperature seems similar (Fig. 1 a and c), but at a high pH, the curves differ (Fig. 1 b and d). Therefore, the firming rate seems to depend mainly on the levels of pH and temperature. The MGR for both constant- and cycled-temperature ramp measurements decreased in the following order: F > E > B > A > H > G > D > C. This trend showed that pH had the strongest effect on MGR, followed by the temperature and $[Ca^{2+}]$ in turn. All three factors plus the interaction of pH and temperature were found to have a significant effect on the MGR for cycled-temperature ramp measurements ($p < 0.05$), as illustrated in Table 2.

The $t_{MGR}$ for all treatments was in a range of 5–15 min, apart from samples with a high pH (6.4) and at a low temperature (31 °C) (treatments C and D), where it was higher (16–23 min) for both modes of temperature measurement (Fig. 2c). The $t_{MGR}$ for cycled-temperature ramp measurements was significantly affected by pH, temperature, and the interaction of pH and temperature (Table 2), but not by $[Ca^{2+}]$. Considering both MGR and $t_{MGR}$ parameters, the differences between treatments with pH 6.0 was due exclusively to the temperature, whereas, for treatments with pH of 6.4, differences were due to the temperature, $[Ca^{2+}]$, or their interaction. This observation is in agreement with the finding of the differences in the G'/time profiles, as mentioned before. As a parameter, $t_{MGR}$ can be used to decide the appropriate time to deposit or start cooling the base layer to obtain the firmest 3D structure.

The G'/time profile with all the high conditions (40 °C, pH 6.4, 5.7 mM $Ca^{2+}$) (treatment H) under constant-temperature mode reached a

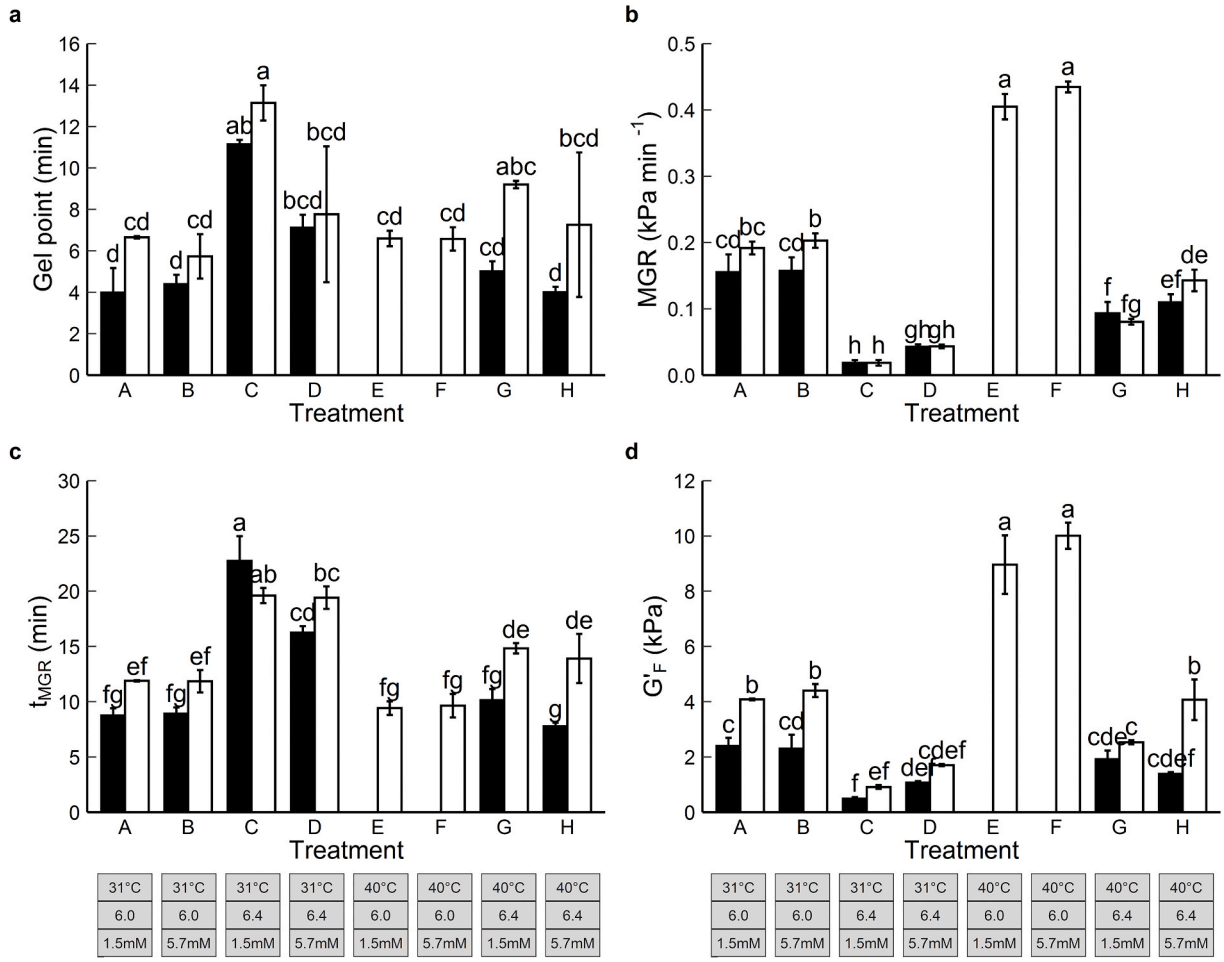


**Fig. 2.** Rennet gelation properties of rennet-treated milk protein dispersions, gel point (a), MGR= maximum gel rate (b), $t_{MGR}$= time to maximum gel rate (c), and $G'_F$= final value of storage modulus measured (d). Constant-temperature mode and cycled-temperature ramp measurements are denoted by black and white bars, respectively. Conditions of each treatment are indicated in the bottom side of the figure, with temperature, pH, and [$Ca^{2+}$] values from top to bottom. Presented values are the mean values of triplicate batches; error bars represent standard deviations of the mean. Treatments not sharing any letters (a–h) differ significantly ($p < 0.05$).

plateau value (G' ~ 1.3 kPa) after ~ 30 min, whereas the same conditions but with low temperature (31 °C) (treatment D) did not reach a similar value within the time of the measurement. Such a trend is consistent with the findings of previous studies showing that increasing temperature promotes a more rapid fusion of para-casein micelles (Mishra et al., 2005). Similar, when increasing the [$Ca^{2+}$] from 1.57 mM to 5.7 mM, at 31 °C and a high pH (6.4) (treatment C to D), contributed to more rapid coagulation. Higher [$Ca^{2+}$] promotes gelation by promoting cross-linking of the para-casein micelles and by charge neutralisation (Fox et al., 2017). However, the effect of increasing [$Ca^{2+}$] depends on the pH, as mentioned before. It appears that lowering the pH to 6.0 contributes more to enhance the coagulation of casein micelles than restoring [$Ca^{2+}$] in the serum of milk protein dispersion in this study.

For 3DFP based on rennet gelation, $G'_F$ is a critical parameter. It indicates the strength of the printed gel structure to withstand additional successively deposited layers without fracturing or bulging. For all treatments, $G'_F$ was higher when measurements were performed using the cycled-temperature ramp than a constant-temperature mode. The higher values with the cycled-temperature ramp were due to the increase in the gel firming rate during cooling. However, the gel firming rate during cooling was different between treatments within the cycled-temperature ramp measurements; for that reason, $G'_F$ was significantly affected by pH, temperature, [$Ca^{2+}$], and the interaction of pH and temperature (Table 2). At a low pH (6.0) and high temperature (40 °C) (treatments E and F), $G'_F$ had the highest values. Therefore, these conditions appear to be optimal to obtain self-supporting structures.

When using the cycled-temperature ramp, pH was the most critical factor affecting the rennet gelation of the milk protein dispersions as it influenced all the rennet gelation parameters. The significant influence of pH can be explained on the basis that lowering pH (from 6.4 to 6.0) enhances chymosin activity, reduces electrostatic repulsion of micelles, increases [$Ca^{2+}$], and thereby reduces gelation time and promotes the aggregation of the para-casein micelles (Fox et al., 2017; Horne & Lucey, 2017). The temperature was also a critical factor, but only for parameters post GP, i.e., MGR, $t_{MGR}$, $G'_F$, as dispersions had the same starting temperature (25 °C) for all treatments. [$Ca^{2+}$] only affected the rennet gelation parameters of treatments with pH 6.4 and a gelation temperature of 31 °C. This is in agreement with the [$Ca^{2+}$] effect, depending on the temperature and pH, as mentioned previously.

Based on these findings, the rennet gelation of the control milk protein dispersion, pH (6.4) and [$Ca^{2+}$] (1.5 mM), at 31 °C is unlikely to be suitable for 3D printing, as structure formation time and the firmness rate of the formed structure are relatively slow. Nevertheless, a lower pH (6.0) and higher temperature (40 °C) led to a more rapid gelation rate with higher strength; therefore, a gel created using these conditions is potentially suitable for extrusion 3D printing. In Fig. 3, a cylinder of the gel formed using the milk protein dispersion prepared at pH 6.0, [$Ca^{2+}$] = 1.5 mM, and 40 °C using the cycled-temperature ramp can be observed. The gel was formed on the rheometer following the same

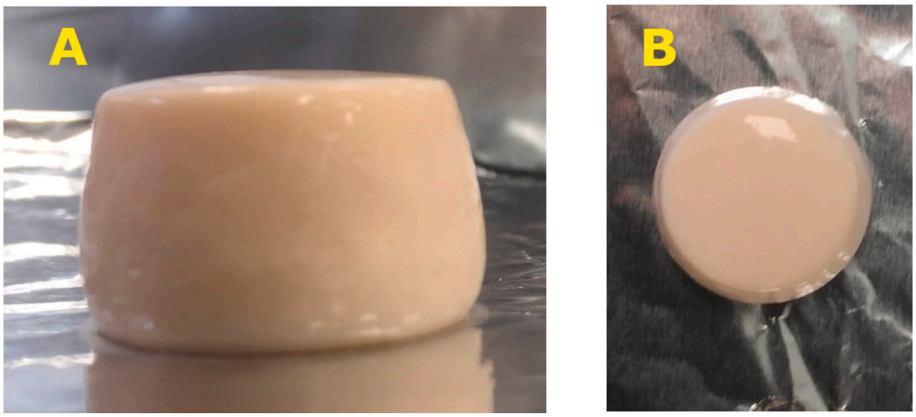


**Fig. 3.** Side (a) and top (b) view of the gel prepared from the milk protein dispersion using the conditions pH 6.0, [$Ca^{2+}$] = 1.5 mM, and 40 °C after decreasing the temperature to 15 °C us-ing the cy-cled-tem-per-a-ture ramp method. The gel was elaborated in the rheometer's bob and cut with a 20 mL syringe with the tip removed.

methodology as mentioned in section 2.6 but without using the bob geometry. After cooling to 15C , a 20 mL syringe with the tip removed was used to take a sample of the core gel out of the cup. This gel shows the potential of milk protein dispersions to form 3D self-supporting gels. However, further studies on the viscosity of the dispersion and mechanical strength of gelled dispersion, syneresis post gelation and printing will be undertaken. These parameters need to be understood and considered for the design and development of a printer, to successfully print a dairy formulation using rennet-induced gelation.

## 4. Conclusions

A distinguishing feature of the cycled-temperature ramp measurements was the significant increase in G' during cooling, and consequently, the significantly higher $G'_F$ for all treatments compared to the constant-temperature mode of measurement. All three factors affected rennet gelation parameters, with the effect of pH being the most pronounced and that of [$Ca^{2+}$] being the least significant and dependent on pH and temperature. Overall, dispersions with pH 6.0 at a temperature of 40 °C, subjected to a cycled-temperature ramp, had the highest gel firming rates and acquired a firm gel strength (~8–9 kPa) by the end of the process. Consequently, they are potentially suited to the formation of rennet-induced 3D food-based structures. However, further studies on viscosity, characteristics of the dispersions and texture properties of the structures are required for the optimisation of the 3D printing process.

## CRediT authorship contribution statement

**Ricardo Uribe-Alvarez:** Conceptualization, Methodology, Investigation, Data curation, Writing. **Norah O'Shea:** Conceptualization, Methodology, Review. **Craig P. Murphy:** Review. **Caroline Coleman-Vaughan:** Review. **Timothy P. Guinee:** Conceptualization, Methodology, Data curation, Review.

## Declaration of competing interest

The authors declare that they have no known competing financial interests or personal relationships that could have appeared to influence the work reported in this paper.

## Acknowledgements

The research was funded by the Department of Agriculture, Food and the Marine under the Food Institutional Research Measure (FIRM) "Exploitation of dairy ingredients in the development of 3 Dimensional Structured Dairy Snacks" 17/F/246 and the Walsh Scholarship programme.

## Appendix A. Supplementary data

Supplementary data to this article can be found online at https://doi.org/10.1016/j.foodhyd.2020.106542.

## References

Agarwal, S., Beausire, R. L. W., Patel, S., & Patel, H. (2015). Innovative uses of milk protein concentrates in product development. *Journal of Food Science, 80*(S1), A23–A29. https://doi.org/10.1111/1750-3841.12807

Augustin, M. A., & Clarke, P. T. (2011). Dry milk ingredients. In *Dairy ingredients for food processing* (pp. 141–159). Wiley-Blackwell. https://doi.org/10.1002/9780470959169.ch6.

Bot, F., Crowley, S. V., & O'Mahony, J. A. (2020). Solubility enhancement of milk protein isolate by sodium caseinate addition: Comparison between wet- and dry-blending approaches. *International Dairy Journal, 105*, 104661. https://doi.org/10.1016/j.idairyj.2020.104661

Corredig, M., & Salvatore, E. (2016). Enzymatic coagulation of milk. In P. L. H. McSweeney, & J. A. O'Mahony (Eds.), *Advanced dairy chemistry* (pp. 287–307). Springer New York. https://doi.org/10.1007/978-1-4939-2800-2_11.

Crowley, S. V., Boudin, M., Chen, B., Gazi, I., Huppertz, T., Kelly, A. L., & O'Mahony, J. A. (2015a). Stability of milk protein concentrate suspensions to in-container sterilisation heating conditions. *International Dairy Journal, 50*, 45–49. https://doi.org/10.1016/j.idairyj.2015.05.009

Crowley, S. V., Desautel, B., Gazi, I., Kelly, A. L., Huppertz, T., & O'Mahony, J. A. (2015b). Rehydration characteristics of milk protein concentrate powders. *Journal of Food Engineering, 149*, 105–113. https://doi.org/10.1016/j.jfoodeng.2014.09.033

Dalgleish, D. G. (1983). Coagulation of renneted bovine casein micelles: Dependence on temperature, calcium ion concentration and ionic strength. *Journal of Dairy Research, 50*(3), 331–340. https://doi.org/10.1017/S0022029900023165

Dalgleish, D. G., & Law, A. J. R. (1988). pH-Induced dissociation of bovine casein micelles. I. Analysis of liberated caseins. *Journal of Dairy Research, 55*(4), 529–538. https://doi.org/10.1017/S0022029900033306

Dalgleish, D. G., & Law, A. J. R. (1989). pH-Induced dissociation of bovine casein micelles II. Mineral solubilisation and its relation to casein release. *Journal of Dairy Research, 56*(5), 727–735. https://doi.org/10.1017/S0022029900029290

Derossi, A., Caporizzi, R., Azzollini, D., & Severini, C. (2018). Application of 3D printing for customised food. A case on the development of a fruit-based snack for children. *Journal of Food Engineering, 220*, 65–75. https://doi.org/10.1016/j.jfoodeng.2017.05.015

Fox, P. F., Guinee, T. P., Cogan, T. M., & McSweeney, P. L. H. (2017). Enzymatic coagulation of milk. In *Fundamentals of cheese science* (pp. 185–229). Springer US. https://doi.org/10.1007/978-1-4899-7681-9_7.

Gazi, I., & Huppertz, T. (2015). Influence of protein content and storage conditions on the solubility of caseins and whey proteins in milk protein concentrates. *International Dairy Journal, 46*, 22–30. https://doi.org/10.1016/j.idairyj.2014.09.009

Godoi, F. C., Prakash, S., & Bhandari, B. R. (2016). 3d printing technologies applied for food design: Status and prospects. *Journal of Food Engineering, 179*, 44–54. https://doi.org/10.1016/j.jfoodeng.2016.01.025

Guinee, T. P., O'Kennedy, B. T., & Kelly, P. M. (2006). Effect of milk protein standardization using different methods on the composition and yields of cheddar cheese. *Journal of Dairy Science, 89*(2), 468–482. https://doi.org/10.3168/jds.S0022-0302(06)72110-5

Gulati, A., Hennessy, D., O'Donovan, M., McManus, J. J., Fenelon, M. A., & Guinee, T. P. (2019). Dairy cow feeding system alters the characteristics of low-heat skim milk

powder and processability of reconstituted skim milk. *Journal of Dairy Science, 102* (10), 8630–8647. https://doi.org/10.3168/jds.2018-15884

Horne, D. S., & Lucey, J. A. (2017). Rennet-induced coagulation of milk. In P. L. H. McSweeney, P. F. Fox, P. D. Cotter, & D. W. B. T.-C. (Fourth E. Everett (Eds.), *Cheese* (pp. 115–143). Elsevier. https://doi.org/10.1016/B978-0-12-417012-4.00005-3.

ISO. (2008). Dried milk and dried milk products - Determination of fat content - Gravimetric method (Reference method). *ISO 1736:2008 [IDF 9:2008]*.

ISO. (2014). Milk and milk products - Determination of nitrogen content - Part 1: Kjeldahl principle and crude protein calculation. *ISO 8968-1:2014 [IDF 20-1:2014]*.

Kern, C., Weiss, J., & Hinrichs, J. (2018). Additive layer manufacturing of semi-hard model cheese: Effect of calcium levels on thermo-rheological properties and shear behavior. *Journal of Food Engineering, 235*, 89–97. https://doi.org/10.1016/j.jfoodeng.2018.04.029

Le Tohic, C., O'Sullivan, J. J., Drapala, K. P., Chartrin, V., Chan, T., Morrison, A. P., … Kelly, A. L. (2018). Effect of 3D printing on the structure and textural properties of processed cheese. *Journal of Food Engineering, 220*, 56–64. https://doi.org/10.1016/j.jfoodeng.2017.02.003

Lille, M., Nurmela, A., Nordlund, E., Metsä-Kortelainen, S., & Sozer, N. (2018). Applicability of protein and fiber-rich food materials in extrusion-based 3D printing. *Journal of Food Engineering, 220*, 20–27. https://doi.org/10.1016/j.jfoodeng.2017.04.034

Lin, Y., Kelly, A. L., O'Mahony, J. A., & Guinee, T. P. (2016). Fortification of milk protein content with different dairy protein powders alters its compositional, rennet gelation, heat stability and ethanol stability characteristics. *International Dairy Journal, 61*, 220–227. https://doi.org/10.1016/j.idairyj.2016.06.010

Lipton, J., Arnold, D., Nigl, F., Lopez, N., Cohen, D., Norén, N., & Lipson, H. (2010). Multi-material food printing with complex internal structure suitable for conventional post-processing. *Solid Freeform Fabrication Symposium*, 809–815.

Lipton, J., Cutler, M., Nigl, F., Cohen, D., & Lipson, H. (2015). Additive manufacturing for the food industry. *Trends in Food Science & Technology, 43*(1), 114–123. https://doi.org/10.1016/j.tifs.2015.02.004

Liu, Z., Bhandari, B., Prakash, S., Mantihal, S., & Zhang, M. (2019). Linking rheology and printability of a multicomponent gel system of carrageenan-xanthan-starch in extrusion based additive manufacturing. *Food Hydrocolloids, 87*, 413–424. https://doi.org/10.1016/j.foodhyd.2018.08.026

Liu, Y., Liu, D., Wei, G., Ma, Y., Bhandari, B., & Zhou, P. (2018). 3D printed milk protein food simulant: Improving the printing performance of milk protein concentration by incorporating whey protein isolate. *Innovative Food Science & Emerging Technologies, 49*, 116–126. https://doi.org/10.1016/j.ifset.2018.07.018

Liu, Y., Yu, Y., Liu, C., Regenstein, J. M., Liu, X., & Zhou, P. (2019). Rheological and mechanical behavior of milk protein composite gel for extrusion-based 3D food printing. *Lebensmittel-Wissenschaft & Technologie, 102*, 338–346. https://doi.org/10.1016/j.lwt.2018.12.053

Liu, Z., Zhang, M., Bhandari, B., & Wang, Y. (2017). 3D printing: Printing precision and application in food sector. *Trends in Food Science & Technology, 69*, 83–94. https://doi.org/10.1016/j.tifs.2017.08.018

Lucey, J. A. (2002). Formation and physical properties of milk protein gels. *Journal of Dairy Science, 85*(2), 281–294. https://doi.org/10.3168/jds.S0022-0302(02)74078-2

Lucey, J. A., & Singh, H. (1997). Formation and physical properties of acid milk gels: A review. *Food Research International, 30*(7), 529–542. https://doi.org/10.1016/S0963-9969(98)00015-5

Lucey, J. A., Teo, C. T., Munro, P. A., & Singh, H. (1997). Rheological properties at small (dynamic) and large (yield) deformations of acid gels made from heated milk. *Journal of Dairy Research, 64*(4), 591–600. https://doi.org/10.1017/S0022029997002380

Mishra, R., Govindasamy-Lucey, S., & Lucey, J. A. (2005). Rheological properties of rennet-induced gels during the coagulation and cutting process: Impact of processing conditions. *Journal of Texture Studies, 36*(2), 190–212. https://doi.org/10.1111/j.1745-4603.2005.00011.x

Morrin, S. T., Lane, J. A., Marotta, M., Bode, L., Carrington, S. D., Irwin, J. A., & Hickey, R. M. (2019). Bovine colostrum-driven modulation of intestinal epithelial cells for increased commensal colonisation. *Applied Microbiology and Biotechnology, 103*(6), 2745–2758. https://doi.org/10.1007/s00253-019-09642-0

Ross, M. M., Kelly, A. L., & Crowley, S. V. (2019). Chapter 7 - potential applications of dairy products, ingredients and formulations in 3D printing. In F. C. Godoi, B. R. Bhandari, S. Prakash, & M. Zhang (Eds.), *Fundamentals of 3D food printing and applications* (pp. 175–206). Academic Press. https://doi.org/10.1016/B978-0-12-814564-7.00007-9.

Schutyser, M. A. I., Houlder, S., de Wit, M., Buijsse, C. A. P., & Alting, A. C. (2018). Fused deposition modelling of sodium caseinate dispersions. *Journal of Food Engineering, 220*, 49–55. https://doi.org/10.1016/j.jfoodeng.2017.02.004

Sinaga, H., Bansal, N., & Bhandari, B. (2017). Gelation properties of partially renneted milk. *International Journal of Food Properties, 20*(8), 1700–1714. https://doi.org/10.1080/10942912.2016.1193515

Singh, H. (2009). Protein interactions and functionality of milk protein products. In *Dairy-derived ingredients* (pp. 644–674). Elsevier. https://doi.org/10.1533/9781845697198.3.644.

Sun, J., Zhou, W., Yan, L., Huang, D., & Lin, L. Y. (2018). Extrusion-based food printing for digitalised food design and nutrition control. *Journal of Food Engineering, 220*, 1–11. https://doi.org/10.1016/j.jfoodeng.2017.02.028

Udabage, P., Puvanenthiran, A., Yoo, J. A., Versteeg, C., & Augustin, M. A. (2012). Modified water solubility of milk protein concentrate powders through the application of static high pressure treatment. *Journal of Dairy Research, 79*(1), 76–83. https://doi.org/10.1017/S0022029911000793

Van Vliet, T., Lakemond, C. M. M., & Visschers, R. W. (2004). Rheology and structure of milk protein gels. *Current Opinion in Colloid & Interface Science, 9*(5), 298–304. https://doi.org/10.1016/j.cocis.2004.09.002

Vancauwenberghe, V., Verboven, P., Lammertyn, J., & Nicolaï, B. (2018). Development of a coaxial extrusion deposition for 3D printing of customisable pectin-based food simulant. *Journal of Food Engineering, 225*, 42–52. https://doi.org/10.1016/j.jfoodeng.2018.01.008

Walstra, P., & Van Vliet, T. (1986). The physical chemistry of curd making. *Netherlands Milk and Dairy Journal, 40*, 241–259.

Wegrzyn, T. F., Golding, M., & Archer, R. H. (2012). Food layered manufacture: A new process for constructing solid foods. *Trends in Food Science & Technology, 27*(2), 66–72. https://doi.org/10.1016/j.tifs.2012.04.006

Zhu, S., Stieger, M. A., van der Goot, A. J., & Schutyser, M. A. I. (2019). Extrusion-based 3D printing of food pastes: Correlating rheological properties with printing behaviour. *Innovative Food Science & Emerging Technologies, 58*, 102214. https://doi.org/10.1016/j.ifset.2019.102214

Zoon, P., Vliet, T. van, & Walstra, P. (1988a). Rheological properties of rennet-induced skim milk gels. 1. Introduction. *Netherlands Milk and Dairy Journal, 42*, 249–269.

Zoon, P., Vliet, T. van, & Walstra, P. (1988b). Rheological properties of rennet-induced skim milk gels. 2. The effect of temperature. *Netherlands Milk and Dairy Journal, 42*, 271–294.